PHYSICAL REVIEW B VOLUME 22, NUMBER 6 15 SEPTEMBER 1980

Experimental energy-band dispersions, critical points, and spin-orbit splittings for GaSb using angle-resolved photoemission

T.-C. Chiang and D. E. Eastman
IBM Thomas J. Watson Research Center, Yorktown Heights, New York 10598
(Received 7 December 1979)

We have determined energy-band dispersions $E(\vec{k})$ and critical points for GaSb using angle-resolved-photoemission techniques. With a normal emission configuration and photon energies between 24 and 95 eV, the valence-band dispersions $E(\vec{k})$ have been obtained along the Γ-K-X direction, with the spin-orbit splitting $\Delta_0(\Gamma_8$-$\Gamma_7)$ clearly observed. With an off-normal emission configuration, we have also determined the valence-band critical-point energies at the L point, with the spin-orbit splitting $\Delta_1(L_{4,5}$-$L_6)$ clearly observed. Experimental valence-band critical-point energies at Γ, X, and L are compared with recent theoretical results. Using published transition energies determined from reflectance measurements, we have also obtained the low-lying conduction-band critical-point energies. These valence- and conduction-band critical-point energies are tabulated to facilitate comparisons with other experimental and theoretical results.

I. INTRODUCTION

Electronic band structures of single crystals are of fundamental importance in solid-state physics. We report here the experimental valence-band structure of GaSb using angle-resolved photoemission with synchrotron radiation. GaSb is a III-V compound with a band structure similar to those of the more familiar Si, Ge, and GaAs. However, due to the large atomic number of Sb, relativistic effects (e.g., spin-orbit interaction) are much more important for GaSb.[1] Thus, a measurement of the band structure of GaSb should provide a test for theoretical treatments of relativistic effects.

Previous experimental studies in determining the valence-band structure of GaSb include x-ray photoemission spectroscopy (XPS)[2] and reflectance[3] measurements. However, such XPS results are not very accurate since valence critical-point energies are extracted from broad, sometimes poorly defined geometrical features in the spectra which reflect density-of-states features. In particular, the spin-orbit splitting, being of the order of 0.5 eV, cannot be extracted from the data reliably. Reflectance measurements, on the other hand, can yield quite accurate transition energies. However, due to the limited number of clearly identifiable transitions and a lack of information concerning their origin, the valence-band structure of GaSb has been only partially determined.

In a previous publication,[4] we have demonstrated simple techniques for experimentally determining valence-band structures using angle-resolved photoemission, and consequently, we have been able to obtain detailed valence-band dispersions $E(\vec{k})$ and lifetime broadenings for GaAs. Relativistic effects are relatively small for GaAs and we have not been able to observe the spin-orbit splittings directly in that case. In the present experiment, we apply the same techniques to GaSb. Even in this more complicated case, it has proven to be a straightforward matter to determine the valence-band dispersion. In particular, we have observed directly the spin-orbit splittings at $L_{4,5} - L_6$ and $\Gamma_8 - \Gamma_7$; all the valence critical-point energies at Γ, X, and L (except X_7) are obtained directly.

The outline of this paper is as follows: Experimental procedures are described briefly in Sec. II. Results are discussed in Sec. III and valence critical-point energies are tabulated and compared with other experimental and theoretical values. Using the transition energies obtained in Ref. 3, we also tabulate the energies of the low-lying conduction-band critical points to facilitate future theoretical and experimental studies of GaSb.

II. EXPERIMENTAL

GaSb has the fcc zinc-blende crystal structure with a lattice constant $a = 6.10$ Å; the cleavage plane is $\{110\}$. The main symmetry directions are [110] (Γ-K-X). [100] (Γ-Δ-X), [111] (Γ-Λ-L) and their equivalent directions; a picture of the Brillouin zone with the critical points can be found in standard textbooks.[5] Important dimensions of the Brillouin zone are $\Gamma KX = \sqrt{2}\,(2\pi/a) = 1.46$ Å^{-1}, $\Gamma\Delta X = 2\pi/a = 1.03$ Å^{-1}, and $\Gamma\Lambda L = \sqrt{3/4}\,(2\pi/a) = 0.892$ Å^{-1}. Single crystals of p-type Zn-doped (2×10^{18} carriers/cm^3) GaSb were cleaved in an ultrahigh vacuum ($\sim 1\times10^{-10}$ Torr) experimental chamber to expose the (110) face.

The experiment was done at the Physical Sciences

Laboratory at the University of Wisconsin-Madison using synchrotron radiation from the 240-MeV storage ring as the light source. Experimental details were identical to those described before for our GaAs studies.[4] In brief, a cylindrical mirror analyzer with 4° (full-angle) angular resolution was used. The system energy resolution was 0.2–0.5 eV in the photon energy range $24 \leq h\nu \leq 95$ eV. A mixed polarizarion was always used such that all valence states are excited regardless of symmetry. Samples were kept at room temperature during the measurements.

III. RESULTS AND DISCUSSION

The techniques used to obtained valence $E(\vec{k})$ dispersions from photoelectron-energy distributions have been explained in detail in Ref. 4; the following description gives a brief summary.

A. Normal emission from GaSb (110)

Normal emission photoelectron-energy distribution curves (unnormalized) as a function of photon energy $h\nu$ are shown in Fig. 1. Long- and short-dashed curves indicate primary-cone emission and secondary-cone and surface umklapp emission peaks, respectively (see below). Broad features A and A' (they are cut off in some spectra by the frame of the figure) are due to Ga and Sb $M_{4,5}\,VV$ Auger transitions, respectively. Some spectra ($h\nu = 25$–31 eV) are truncated to avoid confusion due to strong core-level emission from the second-order light from our monochromator. The initial energy E_i is referenced to the valence-band maximum E_v. The general $h\nu$-dependent behaviors of these peaks are very similar to those for GaAs.[4] At the relatively high photon energies used here ($h\nu \gtrsim 24$ eV), the photoemission spectral peaks can be roughly classified into two categories: primary-cone emission peaks and secondary-cone and surface umklapp emission peaks.[4,6] The primary-cone emission peaks are dispersive with respect to $h\nu$ and are relatively more intense. The final states for these excitations usually can be well described by a lifetime-broadened free-electron dispersion which is shifted down by the inner potential. In this case, the parallel and perpendicular components of the electron momentum inside the crystal can be determined by simple kinematic relations

$$\hbar k_{\parallel} = 0 \tag{1}$$

and

$$\hbar k_{\perp} = [2m(E_i + h\nu - E_0)]^{1/2}, \tag{2}$$

where $k_{\perp}$ is defined in the extended zone scheme, E_i is the measured initial-state energy and E_0

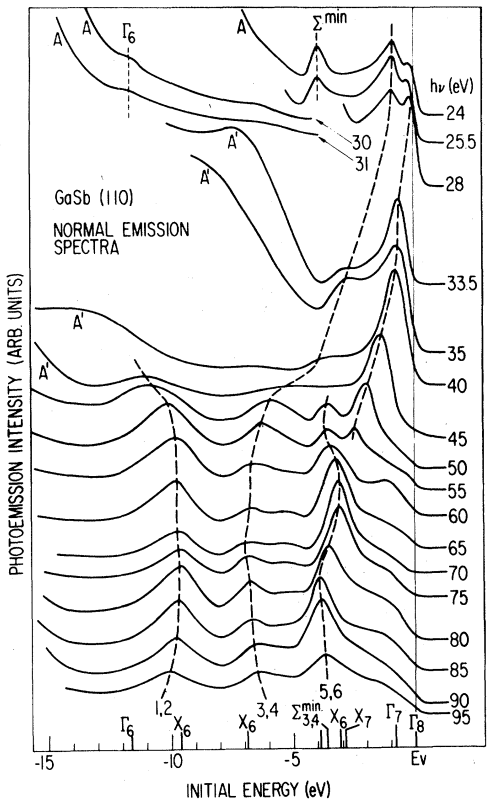

FIG. 1. Angle-resolved photoelectron-energy distribution curves for GaSb (110) as a function of photon energy $h\nu$. The initial energy is referred to the valence-band maximum E_v. Long- and short-dashed curves indicate primary-cone and secondary-cone and surface umklapp emission peaks, respectively. A and A' are emission features (they are cut off in some spectra by the frame of the figure) due to Ga and Sb $M_{4,5}VV$ Auger transitions, respectively. The positions of the relevant critical points are indicated near the bottom of the figure.

is the energy of the "bottom of the muffin-tin." All energies are references to the valence-band maximum E_v. E_0 can be deduced from the normal emission data[4]; the value is equal to the calculated value[7] of −6.92 eV within experimental uncertainty. Using primary-cone emission peaks 1–8 in Fig. 1 and Eqs. (1) and (2), $E_i(\vec{k})$ dispersions for corresponding valence bands 1–8 along the Γ-K-X direction are obtained as shown in Fig. 2. Diamonds, circles, and squares denote data points with $\Gamma KX < k_{\perp} < 2\Gamma KX$, $2\Gamma KX < k_{\perp} < 3\Gamma KX$, and $3\Gamma KX < k_{\perp} < 4\Gamma KX$, respectively. Due to different orbital characters for the spin-orbit-split members in a given doublet (bands 3 and 4, 5 and 6) one member may have stronger emission intensity than the other in a given range of $h\nu$, thus resulting in the observation of only one broad peak for a doublet for these conditions. A reliable theoretical-

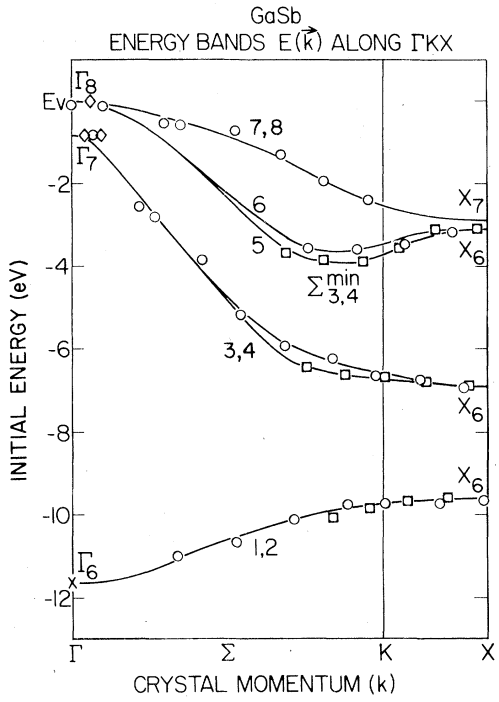

FIG. 2. Experimental band dispersions for GaSb along Γ-K-X. Diamonds, circles, and squares are data points obtained using primary-cone emission peaks with $\Gamma KX < k_\perp < 2\Gamma KX$, $2\Gamma KX < k_\perp < 3\Gamma KX$, and $3\Gamma KX < k_\perp < 4\Gamma KX$, respectively. The data point (cross) at Γ_6 is obtained using secondary-cone and surface umklapp emission-peak positions. Guided by theoretical band dispersions, smooth curves are drawn through the data points to show the general band topology.

intensity calculation is not yet available. Guided by the theoretical band dispersions in Ref. 1, smooth curves are drawn through the data points to denote the "experimental band dispersions." Due to lifetime-broadening effects and finite angular resolution, data points in Fig. 2 are in general uncertain by $|\Delta E_i| \lesssim 0.1$ eV and $|\Delta k_\perp| \lesssim 0.1$ ΓKX.[4] Uncertainties in the peak positions in Fig. 1 due to background and asymmetric line shapes lead to additional $|\Delta E_i| \lesssim 0.2$ eV.

The behavior of the primary-cone emission peaks 1–8 in Fig. 1 can be easily understood. As $h\nu$ increases from 24 to 95 eV, $k_\perp$ increases from less than $2\Gamma KX$ to greater than $3\Gamma KX$, and primary-cone emission peaks from bands 1–8 in Fig. 2 simply follow the dispersion curves according to Eq. (2). The periodic behaviors are quite evident in Fig. 1. The spin-orbit splitting near the valence-band maximum $\Delta_0(\Gamma_8 - \Gamma_7 \simeq 0.8$ eV) is clearly observed in Fig. 1 for $h\nu = 25.5$ eV. Emission from bands 7 and 8 decreases in intensity as $h\nu$ increases to around 70 eV ($k_\perp \sim 3\Gamma KX$), thus the critical point X_7 cannot be located. The smooth

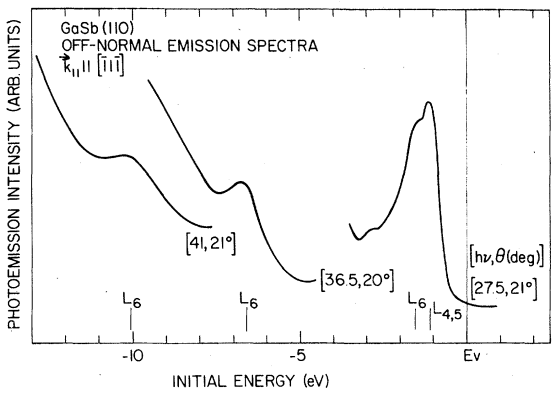

FIG. 3. Off-normal emission spectra from GaSb (110) with $\vec{k}_\parallel \| [\bar{1}\bar{1}]$. The photon energy $h\nu$ and polar emission angle θ were chosen such that primary-cone emission peaks arise from valence-band critical points at L indicated near the bottom of the figure.

curves in Fig. 2 are drawn such that the spin-orbit splitting $\Delta_2(X_7 - X_6)$ is equal to the theoretical values of 0.24 eV.[1]

Turning to the secondary-cone and surface umklapp emission peaks (short-dashed curves in Fig. 1), these are nondispersive with respect to $h\nu$ and are usually weaker than primary-cone peaks. Their positions are in general determined by the one-dimensional valence-band critical

TABLE I. GaSb valence critical-point energies (eV).

Crit. Pt.	ARPES[a]	Theory[b]	XPS[c]	Crit. Pt.[d]
Γ_8	0	0	0	Γ_{15}
Γ_7	−0.82 (7)[e]	−0.76		
Γ_6	−11.64 (10)	−12.00	−11.6 (3)	Γ_1
$L_{4,5}$	−1.10 (7)	−1.00	−1.3 (2)	L_3
L_6	−1.55 (10)	−1.45		
L_6	−6.60 (10)	−6.25	−6.9 (3)	L_1
L_6	−10.06 (10)	−10.17	−10.3 (3)	L_1
X_7	−2.86[f]	−2.37	−2.7 (2)	X_5
X_6	−3.10 (7)	−2.61		
X_6	−6.90 (10)	−6.76	−6.9 (3)	X_3
X_6	−9.62 (10)	−9.33	−9.4 (2)	X_1
$\Sigma_{3,4}^{\min}$	−3.64 (15)	−3.3	−3.8 (2)	$\Sigma_1^{\min}$
$\Sigma_{3,4}^{\min}$	−3.90 (15)	−3.5		

[a] Angle-resolved photoelectron spectroscopy, this work. All energies are referred to the valence-band maximum.

[b] Nonlocal empirical pseudopotential method, Ref. 1.

[c] X-ray photoelectron spectroscopy, Ref. 2.

[d] Critical points in nonrelativistic notation.

[e] Error bound estimates are given in parentheses (in units of last digit given).

[f] Obtained using the experimental value for X_6 and the theoretical value for the spin-orbit splitting $\Delta_2(X_7 - X_6) = 0.24$ eV.

TABLE II. GaSb valence-band spin-orbit splittings (eV).

	ARPES[a]	Reflectance[b]	Theory[c]
$\Delta_0(\Gamma_8-\Gamma_7)$	0.82 (7)	0.756 (10)	0.76
$\Delta_1(L_{4,5}-L_6)$	0.45 (10)	0.430 (10)	0.45
$\Delta_2(X_7-X_6)$			0.24

[a] Angle-resolved photoelectron spectroscopy, this work.
[b] Reference 3.
[c] Nonlocal empirical pseudopotential method, Ref. 1.

points.[4] Peaks labeled Γ_6 and $\Sigma^{\min}$ in Fig. 1 are due to the corresponding critical points Γ_6 and $\Sigma_{3,4}^{\min}$ (the average $\Sigma_1^{\min}$ in the nonrelativistic notation) in Fig. 2. The data point (cross) in Fig. 2 at Γ_6 is obtained this way.

B. Off-normal emission from GaSb (110)

Critical-point energies at L have been obtained using off-normal emission spectra.[4] For primary-cone emission peaks, we have[4]

$$\hbar k_{\parallel} = [2m(E_i + h\nu - e\Phi)]^{1/2} \sin\theta \qquad (3)$$

and

$$\hbar k_{\perp} = \{2m[(E_i + h\nu - e\Phi)\cos^2\theta - V_0]\}^{1/2}, \qquad (4)$$

where $e\Phi = 5.07$ eV is the measured photothreshold (vacuum level minus valence-band maximum), and $V_0 = E_0 - e\Phi = -12.0$ eV is the inner potential ("bottom of the muffin-tin" minus vacuum level). The azimuthal emission angle is chosen such that $\vec{k}_{\parallel} \| [\bar{1}1\bar{1}]$. The photon energy and polar emission angle θ are chosen such that $k_{\perp} \simeq 2\Gamma KX$ and $k_{\parallel} \simeq \Gamma\Lambda L$, i.e., the L point is probed, according to Eqs. (3) and (4). Typical spectra are shown in Fig. 3 with the critical points L_6 and $L_{4,5}$ indicated. The spin-orbit splitting $\Delta_1(L_{4,5}-L_6) \simeq 0.45$ eV (obtained by deconvolution) is clearly observed. The spectra obtained with $\vec{k}_{\parallel}$ along other equivalent directions $[1\bar{1}1]$, $[1\bar{1}\bar{1}]$, and $[\bar{1}11]$ are quite similar except for relative intensity ratios. The critical-point energies obtained from the peak positions are in general uncertain by $|\Delta E_i| \lesssim 0.1$ eV due to finite angular resolution and lifetime-broadening effects.[4]

C. Discussion

Since the band-structure topology of GaSb is well known, it is usually sufficient to know the critical-point energies in lieu of the full $E_i(\vec{k})$

TABLE III. GaSb conduction-band critical-point energies (eV).

Transition and energy (eV)[a]	Experiment[b]	Average[c]	Theory[d]
Γ_{12}^C $E_0''(\Gamma_8^V \to \Gamma_{12}^C)$, 7.9 (1)	7.9 (1)	7.9 (1)	
Γ_8^C $E_0' + \Delta_0'(\Gamma_8^V \to \Gamma_8^C)$, 3.404 (10)	3.404 (10)	3.403 (10)	3.77
$E_0' + \Delta_0' + \Delta_0''(\Gamma_7^V \to \Gamma_8^C)$, 4.160 (20)	3.34 (7)		
Γ_7^C $E_0'(\Gamma_8^V \to \Gamma_7^C)$, 3.191 (5)	3.191 (5)	3.191 (5)	3.44
Γ_6^C $E_0(\Gamma_8^V \to \Gamma_6^C)$, 0.8102	0.8102	0.8102	0.86
$E_0 + \Delta_0(\Gamma_7^V \to \Gamma_6^C)$, 1.559	0.74 (7)		
L_6^C $E_1'(L_{4,5}^V \to L_6^C)$, 5.59 (3)	4.49 (8)	4.49 (6)	4.59
$E_1''(L_6^V \to L_6^C)$, 6.04 (3)	4.49 (10)		
$L_{4,5}^C$ $E_1'(L_{4,5}^V \to L_{4,5}^C)$, 5.46 (2)	4.36 (7)	4.36 (6)	4.43
$E_1''(L_6^V \to L_{4,5}^C)$, 5.90 (7)	4.35 (12)		
L_6^C $E_1(L_{4,5}^V \to L_6^C)$, 2.195 (10)	1.10 (7)	1.09 (6)	1.22
$E_1 + \Delta_1(L_6^V \to L_6^C)$, 2.625 (10)	1.08 (10)		
X_7^C			1.79
X_6^C indirect $(\Gamma_6^C \to X_6^C)$,[e] 0.315 (20)	1.13 (2)	1.13 (2)	1.72

[a] Measured by reflectance (Ref. 3) except for $\Gamma_6^C \to X_6^C$.
[b] Obtained using the ARPES valence critical-point energies in Table I and the transition energies listed. All critical-point energies are for He temperature and referred to the valence-band maximum E_V.
[c] Average of the experimental values.
[d] Nonlocal empirical pseudopotential method, Ref. 1.
[e] Obtained from pressure-measurement and temperature-dependence data, Refs. 8 and 9.

dispersion relations.[4] The experimental valence critical-point energies at Γ, X, and L obtained from Figs. 2 and 3 are listed in Table I together with theoretical and XPS results.[2] The XPS results are labeled according to the nonrelativistic notations in the rightmost column following Ref. 2. The theoretical values were obtained using a nonlocal pseudopotential method which was fit to XPS and reflectance results.[1] The agreement between theoretical and experimental values is generally good. The largest deviation (~0.5 eV) occurs at X_6 and X_7.[3] Values for spin-orbit splittings are listed in Table II. Since the emission intensity of X_7 is much smaller than that of X_6 in both normal and off-normal emission spectra, $\Delta_2(X_7 - X_6)$ has not been determined. Within experimental uncertainty, our values for $\Delta_0(\Gamma_8 - \Gamma_7)$ and $\Delta_1(L_{4,5} - L_6)$ are the same as those obtained from reflectance measurements.[3]

Using our ARPES (angle-resolved photoelectron spectroscopy) results in Table I and the optical transition energies measured by reflectance,[3] a compilation of low-lying conduction-band critical-point energies is given in Table III. Although our ARPES measurements were performed at room temperature and the reflectance measurements were at liquid-He temperature, the observed rigidity of the valence bands with temperature[8] implies that the values in Table III can be regarded as He-temperature values. The value for X_6^C marked "indirect" is obtained using the pressure-dependence measurement of the resistivity[9] and the temperature-dependence coefficients for the conduction bands.[8] Theoretical values[1] are also listed for comparison. It is seen that the theoretical values are larger than the experimental values with the largest deviation (~0.5 eV) occurring at X_6^C.

In summary, one electron valence-band and low-lying conduction-band critical-point energies for GaSb have been accurately determined as given in Tables I and III. These results should serve as a critical test for future theoretical band calculations. This work also demonstrates the utility of the angle-resolved photoemission techniques for general band-structure determinations.

ACKNOWLEDGMENTS

The authors wish to express their appreciation to K. C. Pandey, D. E. Aspnes, F. Himpsel, J. A. Knapp, M. Aono, J. F. van der Veen, A. Marx, and J. J. Donelon for assistance and helpful discussions. We have also benefited from the cooperation of E. M. Rowe and the Synchrotron Radiation Center staff. This work is supported in part by the U. S. Air Force Office of Scientific Research.

[1] J. R. Chelikowsky and M. L. Cohen, Phys. Rev. B 14, 556 (1976).
[2] L. Ley, R. A. Pollak, F. R. McFeely, S. P. Kowalczyk, and D. A. Shirley, Phys. Rev. B 9, 600 (1974).
[3] D. E. Aspnes, C. G. Olsen, and D. W. Lynch, Phys. Rev. B 14, 4450 (1976).
[4] T.-C. Chiang, J. A. Knapp, D. E. Eastman, and M. Aono, Solid State Commun. 31, 917 (1979); T.-C. Chiang, J. A. Knapp, M. Aono, and D. E. Eastman, Phys. Rev. B 21, 3513 (1980).
[5] See, for example, C. Kittel, *Quantum Theory of Solids* (Wiley, New York, 1963), p. 213; R. H. Parmenter, Phys. Rev. 100, 573 (1955).
[6] G. D. Mahan, Phys. Rev. B 2, 4334 (1970).
[7] K. C. Pandey (unpublished).
[8] D. Auvergne, J. Camassel, H. Mathieu, and M. Cardona, Phys. Rev. B 9, 5168 (1974).
[9] B. B. Kosicki, A. Jayaraman, and W. Paul, Phys. Rev. 172, 764 (1968).